BRAIN CONNECTIVITY
Volume 5, Number 4, 2015

DOI: 10.1089/brain.2014.0272

Negative Blood Oxygen Level Dependent Signals During Speech Comprehension

Diana Rodriguez Moreno,[1] Nicholas D. Schiff,[2] and Joy Hirsch[3]

Abstract

Speech comprehension studies have generally focused on the isolation and function of regions with positive blood oxygen level dependent (BOLD) signals with respect to a resting baseline. Although regions with negative BOLD signals in comparison to a resting baseline have been reported in language-related tasks, their relationship to regions of positive signals is not fully appreciated. Based on the emerging notion that the negative signals may represent an active function in language tasks, the authors test the hypothesis that negative BOLD signals during receptive language are more associated with comprehension than content-free versions of the same stimuli. Regions associated with comprehension of speech were isolated by comparing responses to passive listening to natural speech to two incomprehensible versions of the same speech: one that was digitally time reversed and one that was muffled by removal of high frequencies. The signal polarity was determined by comparing the BOLD signal during each speech condition to the BOLD signal during a resting baseline. As expected, stimulation-induced positive signals relative to resting baseline were observed in the canonical language areas with varying signal amplitudes for each condition. Negative BOLD responses relative to resting baseline were observed primarily in frontoparietal regions and were specific to the natural speech condition. However, the BOLD signal remained indistinguishable from baseline for the unintelligible speech conditions. Variations in connectivity between brain regions with positive and negative signals were also specifically related to the comprehension of natural speech. These observations of anticorrelated signals related to speech comprehension are consistent with emerging models of cooperative roles represented by BOLD signals of opposite polarity.

Key words: blood oxygen level dependent signal; coupling; functional connectivity; functional magnetic resonance imaging; speech

Introduction

Language reception and production are the two primary components of human communication. Spoken language is fundamental to human social behavior and language learning starts early in life. Comprehension of speech involves many levels of input processing, from the simplest sound processing to recognizing speech components, assigning meaning to words, and finally, integrating the words into sentences and the sentences within a context of the narrative for the understanding of the speech. Integration of all these processes involves multiple associated brain regions. The neural correlates of these tasks have been extensively studied and canonical language areas in the temporal and frontal cortices are well known. Blood oxygenation level dependent (BOLD) signals acquired by functional magnetic resonance imaging (fMRI) increase with respect to a resting baseline indicating stimulation-induced activation of these regions.

On the other hand, BOLD signals in areas associated with semantic processing have been widely observed as stimulation-induced deactivations with respect to a resting baseline during a wide range of nonsemantic tasks. These regions, collectively designated as a default mode network (DMN), have been also reported in meta-analyses of spontaneous cognition (Biswal et al., 1995; Fox and Raichle, 2007; Gusnard et al., 2001; Mazoyer et al., 2001; Shulman et al., 1997). However, semantic tasks have not typically been associated with deactivations within the DMN regions, and Binder and colleagues (1999) proposed that during conscious passive states like rest, subjects engaged in task-unrelated thoughts that were essentially semantic, and therefore, semantic tasks do not show deactivation of the DMN as other tasks

[1]Department of Psychiatry, Yale School of Medicine, New Haven, Connecticut.
[2]Departments of Neurology and Neuroscience, Weill Medical College, Cornell University, New York, New York.
[3]Departments of Psychiatry and Neurobiology, Yale School of Medicine, New Haven, Connecticut.

do. In agreement with this idea, nonsemantic tasks used in language studies (perceptual matching, nonword reading) generally produced deactivations that overlap with the DMN regions (Binder et al., 2005; Mechelli et al., 2003; Rissman et al., 2003; Xiao et al., 2005). Stimulation-induced deactivations observed in the DMN regions would then represent a direct competition for attention and executive resources, where regions that carry out effortful tasks (guided by exogenous signals) suppress regions that carry out task-unrelated thoughts (guided by endogenous signals).

These observations have shifted the focus of functional imaging studies initially from task-induced activations to task-induced deactivations (Buckner et al., 1996; McKiernan et al., 2003). When task-induced activations and deactivations are observed in comparison to a resting baseline, they reflect both positive and negative BOLD signals (above or below the signal of a resting baseline). This is distinguished from signals that are compared to another task and are positive or negative relative to activity in a related contrast. Furthermore, multiple cognitive tasks have been shown to engage anticorrelated positive and negative signals (Anderson et al., 2011; Anticevic et al., 2010; Buckner et al., 2008; Fox et al., 2005; Vincent et al., 2008). Although the roles of brain regions with positive BOLD signals are well studied in receptive language processes (Ackermann and Riecker, 2010; Price, 2012; Zekveld et al., 2006), the putative roles of brain regions with negative BOLD signals relative to a resting baseline and the interaction between these regions are not well appreciated.

So-called deactivations observed in many language studies are the result of comparisons between two conditions. The absence of a resting baseline precludes the distinction of deactivations with negative BOLD signals from those due to different task demands across conditions. For example, to compare semantic processing of content and function words, Diaz and McCarthy (2009) used a working memory task in which nonwords have to be remembered or retrieved and interspersed with words that were task irrelevant. This design, where the baseline condition is a simple task rather than a resting baseline, is optimal to differentiate areas more responsive to function words or content words, but poor at determining which areas elicit a positive or negative BOLD response relative to a baseline. The observed deactivation of the dorsolateral prefrontal cortex for the word condition with respect to the nonword baseline cannot be assumed to correspond to a negative BOLD signal (Diaz and McCarthy, 2009).

Language studies where deactivations correspond to negative BOLD signals with respect to a resting baseline are few (Yoncheva et al., 2010) and usually focused on regions of the DMN (Schafer and Constable, 2009; Seghier and Price, 2009; Snijders et al., 2009). The activation or deactivation of DMN nodes has been shown to vary with task: language tasks that engage episodic memory retrieval activate posterior nodes of the DMN and deactivate the anterior node in the middle prefrontal cortex. Furthermore, language tasks have been shown to recruit nodes in regions of the parietal lobule (Sestieri et al., 2011) or subregions of left angular gyrus (Seghier et al., 2010) that are anatomically separate from the DMN. The interrelationship between activations and deactivations, in summary, has been shown to depend on the task and the specific demands, but remains poorly understood.

In this study, the authors investigate the relationship between stimulation-induced activations and deactivations during levels of speech comprehension. They specifically ask if the intelligibility of a stimulus induces variable signal deactivations. If so, would those deactivations be only located within the DMN system?

Methods

Subjects

Fifteen healthy right-handed subjects, six male, ages 30.5 ± 7.5 years were recruited for this study. Signed consent from the subjects was obtained before participation in the study in accordance with established institutional guidelines at the Columbia University, Cornell University, and at Yale School of Medicine. Data from one subject were discarded due to uncorrectable movement artifacts.

Imaging

All scans were collected on a 1.5-T General Electric magnetic resonance scanner with a standard head coil. The authors used foam to cushion the subjects' head and paper tape across the forehead to assist subjects to remain stable during the scanning sessions. Functional scans consisted of axial single shot echo planar imaging time series (128×128 mm matrix, 21 contiguous slices, field of view = 190 mm, $1.5 \times 1.5 \times 5$ mm voxels, time to repeat = 3000 msec, time to echo = 43 msec, flip angle = 60°) obtained parallel to a line passing through the anterior and posterior commissures. A total of 120 images were acquired in each run. Conventional high-resolution (T1-weighted) images were also acquired along sagittal planes and at the same axial plane locations as the T2*-weighted images.

Study paradigm

The activation paradigm consisted of two separate runs with alternating blocks of stimulation and rest. The auditory stimuli were personal narratives that were prerecorded by a friend or family member. Sentences that narrated an event of the subject's life were employed to enhance engagement during passive listening and simulated natural language. Three segments of the narratives, each lasting 18 sec, were selected for each run. These segments were modified to create three auditory conditions. (i) Natural speech condition: the segment was played as recorded, the content was comprehensible, and sounded like natural speech; (ii) reversed speech condition: the segment was digitally time reversed, so meaning and prosody were removed, and (iii) muffled speech condition: frequency components higher than 400 Hz and lower than 80 Hz were removed by a band-pass filter to preserve fundamental frequency variability, lexical tone, prosody, and speech rate, but rendered the content unintelligible. The stimuli were adjusted to equate for perceived loudness. The nine auditory segments were interleaved with resting baseline (periods of no stimulation), each lasting 18 sec, the first block in a run being a rest, and the order of the conditions was counterbalanced across runs. Each run had 9 additional seconds at the beginning and the end for processing purposes. Subjects wore headphones designed to reduce background scanner noise (Resonance Technology, Inc.). All subjects were instructed to keep their eyes closed and ''listen to the

narratives interspersed between periods of rest.'' These instructions were consistent for all conditions to assure that, over all, rest periods were comparable across conditions. Before the acquisition of the data, 6–10 images were acquired during a typical speech segment to confirm that the subject was able to understand the language over the scanner noise. Subjects were instructed to listen to the stimuli in all cases and were informed that in some cases they might not understand the content. All subjects were queried following each run regarding their experience. In all cases, subjects reported hearing all stimuli, understanding the natural speech, and not understanding the content of the reversed or the muffled speech.

Data analysis

Preprocessing. The first five images from each run were removed and runs were concatenated for preprocessing and analysis. Initial analysis of image quality to discard image artifacts and excessive motion was performed with the CANlab software diagnostic tools (Cognitive and Affective Neuroscience Lab, University of Colorado at Boulder). Image processing and analysis were performed with Statistical Parametric Mapping (SPM)8 software (Wellcome Department of Imaging Neuroscience, University College, London, United Kingdom). Preprocessing steps included normalization to standard MNI space, motion correction using a sync interpolation algorithm, and smoothing with a 6 mm full-width half-maximum Gaussian kernel. The BOLD response was modeled by boxcar functions for each condition (natural, reversed, and muffled speech) that were convolved with the canonical hemodynamic response function. A 160-sec high-pass filter was used to remove low-frequency confounds, and a low-pass filter shaped to match the canonical hemodynamic response function was used to remove unknown temporal autocorrelations. Motion parameters and the global value for each frame and detected spikes using the diagnostic tools were then used as nuisance regressors for subsequent analysis.

BOLD activation analysis. Statistical analysis of each subject's data was based on the general linear model (GLM) with three task regressors (natural, reversed, and muffled conditions), six motion parameters, and a session regressor on each voxel in the entire brain volume. The single-subject contrast images were used for a second-level random effects group analysis. SPM[T] volumes were generated to investigate the effect of listening to all conditions (natural, reversed, and muffled speech) in comparison with the resting baseline and the contrast of natural speech greater than reversed and muffled speech to isolate regions associated with processing of intelligible speech. Individual voxel thresholds were set at $p < 0.001$ ($t \geq 3.79$). To protect against false-positive results, an effective $p \leq 0.02$ corrected threshold was satisfied by using only clusters of 40 or more voxels, as determined by 10,000 Monte Carlo simulations of whole-brain fMRI data with the above parameters using AlphaSim in AFNI (v2009). Visualization and assignments of anatomic labels and MNI coordinates for active regions were performed using xjview toolbox (http://alivelearn.net/xjview).

Block signal averaging. The average of the block signal was calculated for the clusters associated to speech comprehension (natural speech vs. reversed and muffled speech). The time courses for all the voxels in each cluster were used. Each time course was divided into 36-sec segments consisting of 18-sec condition block and its following 18-sec resting block. The resulting (speech + rest) blocks were grouped according to the condition (natural, reversed, and muffled speech). The average time course for all the 36-sec blocks for each condition was calculated using MATLAB.

Psychophysiological interaction analysis. Functional connectivity was assessed using psychophysiological interaction (PPI) analysis. This analysis identifies contributions of one brain region to another brain region that change with the experimental condition. Regions with responses during natural speech that were greater than muffled and reversed speech conditions for the group analysis were combined as a ''comprehension seed'' for the PPI (Uddin et al., 2009). Time-course series were extracted from the composite comprehension seed (network seed) for each participant and summarized as the first principal component across all voxels. The time series were adjusted with respect to the main effect of the stimulation to partial out confounds. The resulting residual signals were convolved with the psychological factor (intelligibility of the speech given by the comparison of natural vs. muffled and reversed speech) to create the PPI regressors (Friston et al., 1997). A GLM was applied with the PPI regressor, the network seed time series, the three experimental task regressors, and the six motion parameters as effects of no interest. SPM *t*-maps were thresholded at $p < 0.001$ ($t \geq 3 > 79$, uncorrected at the voxel level) with clusters the size of 40 voxels.

Results

Positive and negative signals associated with all listening conditions

The conjunction of all speech conditions (natural, reversed, and muffled) compared to resting baseline engaged regions with both positive BOLD signals (Fig. 1 red clusters; Table 1a) and with negative BOLD signals (Fig. 1, blue clusters; Table 1b) with respect to the resting baseline. The positive signals extended over bilateral temporal regions (middle, superior, and transverse gyri), left frontal regions (inferior and precentral gyri), left hippocampal gyrus, and right putamen. As expected, the positive signals included traditional areas for auditory and language processing. The negative signals associated with all speech conditions constituted clusters over bilateral medial, middle, and superior frontal, precuneus in the inferior parietal cortex, anterior, middle, and posterior cingulate gyrus, middle occipital gyrus, left hippocampal gyrus, bilateral parahippocampal gyri, and left thalamus. Most of these clusters have generally been associated with the DMN. As expected for a language task, the lateral temporal cortex, which is usually observed as a negative signal region included in the DMN, was observed here as a positive signal region. Notably, the posterior cingulate cortex (PCC) engaged with the DMN in previous studies was not observed in this contrast.

Positive and negative signals associated with speech comprehension

Speech comprehension, as observed during the natural speech compared to muffled and reversed speech conditions

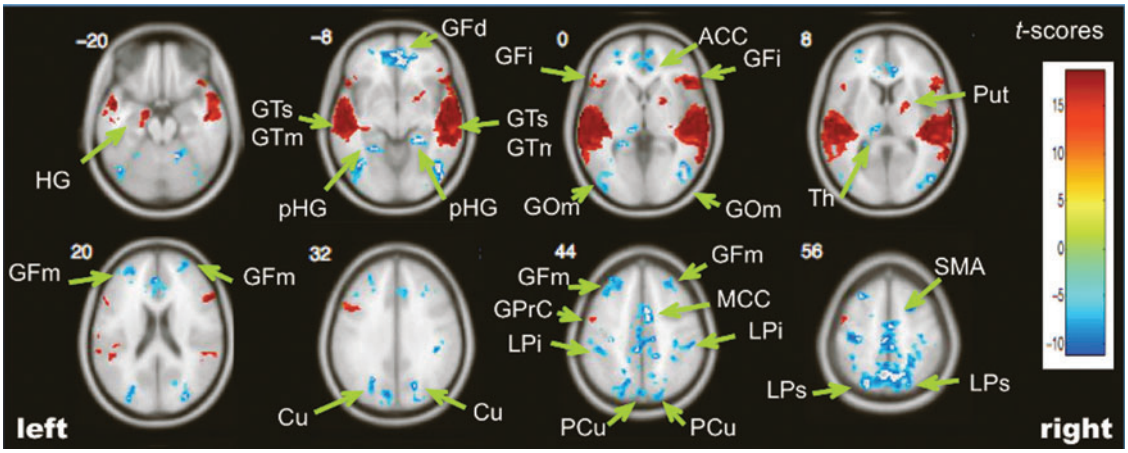

FIG. 1. Main effect of listening to all speech conditions (natural, reversed, and muffled) in comparison to resting baseline (effective corrected threshold $p \leq 0.02$ for cluster size 40, color bar = t-scores). Red: positive signals, cyan: negative signals. ACC, anterior cingulate cortex; Cu, cuneus; GFi, inferior frontal gyrus; GFd, medial frontal gyrus; GFm, middle frontal gyrus; GH, hippocampal gyrus; GOm, middle occipital gyrus; GPrC, precentral gyrus; GTm, middle temporal gyrus; GTs, superior temporal gyrus; LPi, inferior parietal lobule; LPs, superior parietal lobule; MCC, middle cingulate cortex; PCu, precuneus; pHG, parahippocampal gyrus; Put, putamen; SMA, supplementary motor area; Th, thalamus.

(meaningful speech with respect to incomprehensible speech), engaged activated regions (Fig. 2, brain slices in the left, red clusters; Table 2a) and deactivated regions (Fig. 2 left panels, blue clusters; Table 2b) for the comparison of speech conditions. Activated regions included bilateral temporal regions (middle temporal extending to the temporoparietal junction), frontal regions (left inferior and bilateral superior), bilateral parahippocampal gyrus, right hippocampal gyrus, caudate, and thalamus.

The time course and magnitude of the block-averaged BOLD signals of bilateral temporal cortices and left inferior frontal regions are shown in the top row of Figure 2. These graphs confirm the positive BOLD signal (above the resting baseline) for the natural speech condition on the temporal and frontal cortices. The BOLD signal is also positive for the reversed and muffled speech conditions. The amplitude of the positive BOLD signal varies with condition and is higher for the natural speech than for the reversed and muffled speech, and amplitude for reversed speech exceeds that of muffled speech. In addition, the posterior cingulate gyrus and neighboring calcarine extending to the precuneus and cuneus were also observed. The time course for this cluster (Fig. 2, third row, right panel) shows that the BOLD signal is positive (above the resting baseline) for the natural speech condition (red), close to resting baseline for the reversed speech condition (blue), and negative (below the resting baseline) for the muffled condition (green) during the first six initial images corresponding to the task epoch (0–18 sec).

The deactivated regions (Fig. 2, brain slices, left column, blue clusters, and Table 2b) associated with the natural speech in comparison to reversed and muffled speech included frontal regions (bilateral middle and left inferior gyri), parietal regions (bilateral superior, inferior, precuneus, and postcentral gyri), left occipital regions (superior and cuneus), and right insula (see Table 2b for the complete list with MNI coordinates). On the other hand, the frontal eye field areas usually observed in visual attention tasks were not observed here in the passive auditory task.

The time course and magnitude of the BOLD signals of representative regions are shown in the second to bottom rows of Figure 2. Importantly, the graphs show the negative BOLD signals (below the resting baseline) in these regions for the natural speech condition and illustrate that the amplitudes for the negative signals are smaller than those of the positive BOLD signals as expected (Kannurpatti and Biswal, 2004). Therefore, the results can be interpreted as true deactivations of these regions during the natural speech condition rather than a relative difference of natural speech condition in comparison to the reversed and muffled speech conditions. In addition, the BOLD signals during muffled and reversed conditions in these regions are close to baseline levels confirming that these regions are not engaged during the reversed or muffled conditions. Although the graphs shown in Figure 2 correspond to each condition and its following resting baseline for the given region of interest, each region was obtained by the SPM contrast, and therefore, the signal was assumed to reflect a significant change above the average of combined resting baselines.

Summarizing, the global deactivated frontoparietal signals associated with intelligible speech were functionally anticorrelated with the traditional language system.

Functional connectivity of negative signals during language comprehension

To understand the dynamics of these negative signals during processing of intelligible speech, the authors looked at the functional connectivity of all regions associated with language comprehension. They used the comprehensive set of frontoparietal deactivated regions observed for the contrast of natural speech against reversed and muffled speech as a seed for PPI (clusters of negative BOLD signal seen in blue in Fig. 2). These deactivated brain regions increased connectivity with supplementary motor area (SMA) (Table 3a; Fig. 3A, red clusters) and decreased connectivity with the canonical language regions in the middle and superior temporal gyri, and inferior frontal

Table 1. Main Effect of Listening: Passive Listening to All Speech Conditions in Comparison to Resting Baseline

Region	*Anatomical area*	*Brodmann's area*	*T max*	*x*, y, z *(mm)*
a. Listening > Baseline (positive BOLD network)				
Temporal	Superior (L)	22	10.69	−42 −24 8
Temporal	Superior (L)	22	10.52	−48 −30 4
Temporal	Superior (L)	42	11.19	−62 −18 10
Temporal	Superior (R)	22	13.42	52 −14 −6
Temporal	Superior (R)	22	12.71	46 −24 0
Temporal	Superior (R)	22	12.3	62 −22 −2
Frontal	Inferior operculum (L)	45	5.43	−52 18 12
Frontal	Inferior orbitalis (L)	47	6.5	−52 20 −8
Frontal	Precentral (L)	6	5.75	−50 −4 54
Frontal	Precentral (L)	6	5.52	−54 0 48
Frontal	Precentral (L)	6	4.21	−46 −4 46
Frontal	Precentral (L)	9	5.61	−48 12 32
Limbic	Hippocampus (L)	34	6.58	−16 −6 −20
Limbic	Hippocampus (L)	35	4.49	−20 −20 −18
Limbic	Hippocampus (L)		5.27	−24 −12 −16
Sublobar	Putamen (R)		9.78	20 0 4
Sublobar	Putamen (R)		4.22	30 10 −6
b. Listening < Baseline (negative BOLD network)				
Temporal	Middle (R)	37	11.67	44 −66 0
Frontal	Medial orbital (R)	10	9.53	2 52 −8
Frontal	Middle (L)	8	11.32	−28 22 54
Frontal	Middle (R)	10	5.84	28 58 22
Frontal	Middle (L)	10	6.95	−30 38 14
Frontal	Middle (L)	11	5.46	−26 46 2
Frontal	Middle (R)	10	4.68	26 30 38
Frontal	Middle (R)	8	6.29	26 36 50
Frontal	Middle (R)	9	6.09	34 34 38
Frontal	Superior (L)	6	5.62	−16 4 62
Frontal	Superior (L)	6	5.48	−20 0 70
Frontal	Superior (L)	6	3.94	−18 14 64
Frontal	Superior (R)	6	7.54	22 10 58
Frontal	Superior orbital (L)	10	6.72	−26 54 −6
Limbic	Anterior cingulate (R)	32	10.19	8 44 −10
Limbic	Hippocampus (L)		9.12	−22 −40 0
Limbic	Parahippocampal gyrus (L)	19	9.98	−24 −50 −10
Limbic	Parahippocampal gyrus (R)	30	8.87	26 −42 −10
Occipital	Fusiform (L)	19	9.01	38 −68 −12
Occipital	Fusiform (L)	19	6.65	−44 −68 −20
Parietal	Precuneus (L)	7	11.1	−4 −62 58
Parietal	Precuneus (R)	7	11.99	2 −18 74
Sublobar	Thalamus pulvinar (L)		8.31	−12 −26 2
Sublobar	Thalamus pulvinar (L)		4.15	−16 −32 6
Sublobar	Thalamus (L)		4.42	−8 −22 16
Cerebellum	(R)	4, 5	8.68	18 −52 −20

Effective corrected threshold $p \leq 0.02$ for cluster size 40.
x, *y*, *z* = MNI coordinates for activation peak of significant clusters.
BOLD, blood oxygen level dependent.

gyrus (Table 3b; Fig. 3A, blue clusters) during speech comprehension. These brain regions were observed in the contrast of all speech conditions against resting baseline (Fig. 1). Thus, the global deactivated frontoparietal signals associated with intelligible speech processing were functionally less connected with the traditional language system.

Functional connectivity of positive signals during language comprehension

Similarly, the authors used the comprehensive group of activated regions previously observed for the contrast of natural speech greater than reversed and muffled speech as a seed for PPI (clusters of positive BOLD signal seen in red in Fig. 2A) and observed that the activated temporal and inferior frontal regions increased connectivity with the bilateral temporal cortices (middle, superior, and transverse temporal cortex), and with left supramarginal gyrus, left hippocampal gyrus, and right postcentral (Table 4a; Fig. 3B, red clusters). On the other hand, these frontal and temporal activated regions decreased their connectivity to frontal gyrus (medial, middle, and superior frontal gyrus), precuneus in the inferior parietal lobule, medial structures (anterior and posterior

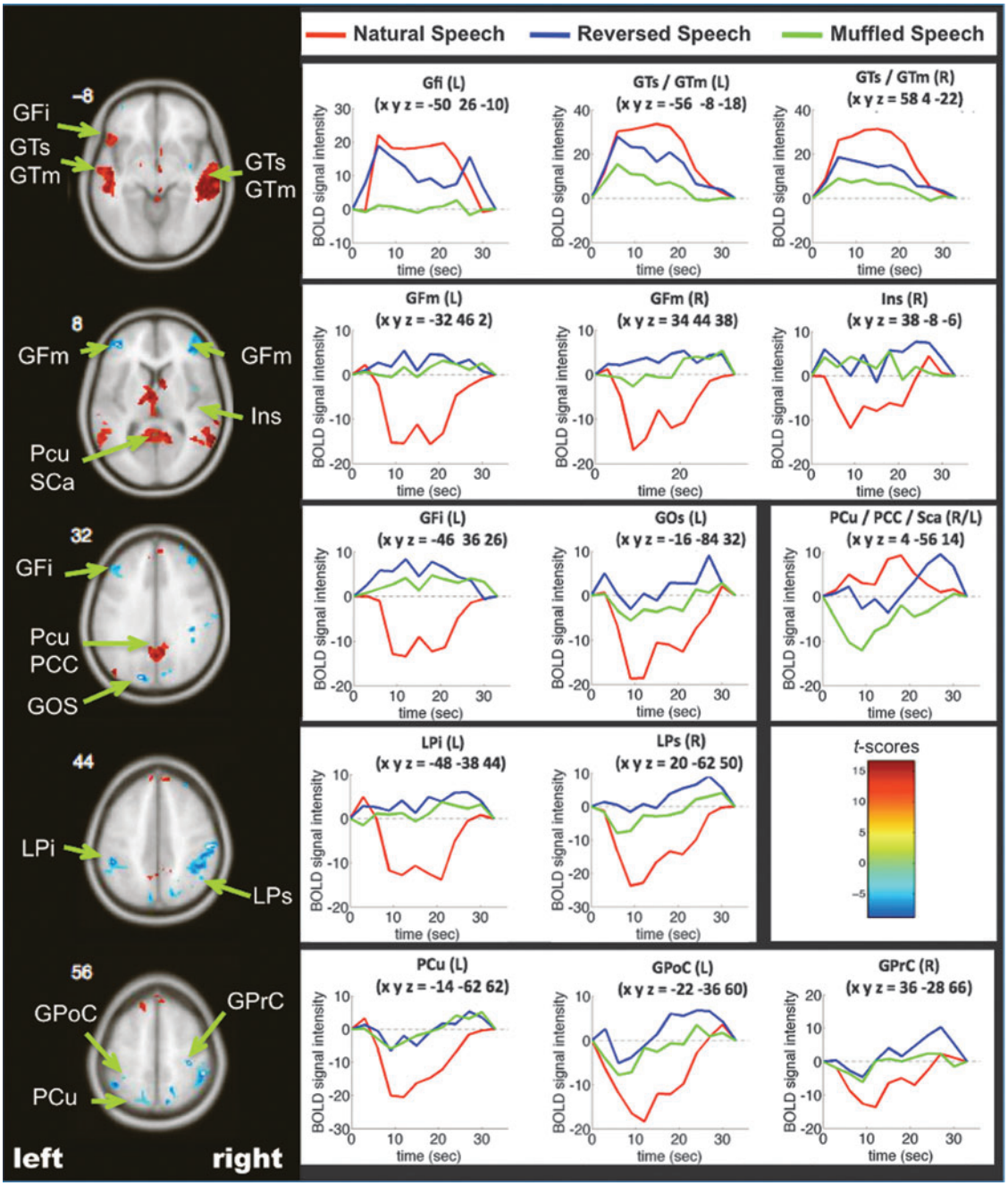

FIG. 2. Main effect of language comprehension (natural speech in comparison to muffled and reversed speech) (effective corrected threshold $p \leq 0.02$ for cluster size 40, color bar = t-scores). Representative brain slices are shown in the left panels. Red: positive signals, cyan: negative signals. The time course for the block-average BOLD signals is shown in the right panels. Signals above the zero baseline correspond to positive BOLD signals relative to a resting baseline. Signals below the zero baseline correspond to negative BOLD signals relative to a resting baseline. Red: natural speech, blue: reversed speech, and green: muffled speech. BOLD, blood oxygen level dependent.

cingulate gyri), and thalamus (Table 4b; Fig. 3B, blue clusters). Most of these areas were observed as deactivations in Figure 1 (ventromedial prefrontal cortex, PCC and posterior inferior parietal lobule) and are usually observed as part of the DMN. Thus, the activated regions associated with speech comprehension appear more connected to areas responsible for low-level auditory processing and less connected to the medial regions when the stimuli are meaningful.

Summarizing, the authors find that the processing of natural meaningful speech involves a constellation of brain regions with negative and positive BOLD signals relative to a resting baseline. While the amplitude of the positive BOLD signal was graded for the three conditions, the amplitude of the negative BOLD signal was not graded and only present during the intelligible speech condition. Regions of positive and negative signals were collectively distinguished by their functional

Table 2. Main Effect of Listening to Intelligible Speech: Passive Listening to Natural Speech in Comparison to Passive Listening to Muffled and Reversed Speech

Region	*Anatomical area*	*Brodmann's area*	*T max*	*x,* y, z *(mm)*
a. Listening to natural speech > Reversed and muffled speech (positive BOLD signal)				
Temporal	Middle (L)	21	8.53	−56 −8 −18
Temporal	Middle (L)	21	7.64	−48 −14 −10
Temporal	Middle (L)	22	7.39	−54 −26 −2
Temporal	Middle (R)	21	11.97	58 4 −22
Temporal	Middle (R)	21	9.78	64 −34 −8
Temporal	Middle (R)	21	9.21	56 −36 −10
Frontal	Inferior orbital (L)	47	5.32	−50 26 −10
Frontal	Inferior orbital (L)	47	4.27	−40 22 −14
Frontal	Inferior triangular (L)	47	5.18	−44 22 −2
Frontal	Superior (L)	8	5.47	−14 36 52
Frontal	Superior (L)	8	4.8	−12 30 58
Frontal	Superior medial (L)	9	6.13	−4 56 38
Frontal	Superior medial (L)	9	4.7	−2 46 38
Frontal	Superior medial (R)	8	5.73	6 36 60
Frontal	Superior medial (R)	9	4.89	4 52 40
Limbic	Parahippocampal (L)	28	6.12	−20 −20 −20
Limbic	Parahippocampal (R)	25	5.97	24 −24 −22
Limbic	Hippocampal (R)	35	5.82	32 −18 −26
Limbic	Hippocampal (R)	35	5.66	30 −16 −16
Occipital	Calcarine/precuneus (R)	23	8.56	4 −56 14
Sublobar	Amygdala (L)		7.14	−16 −2 −14
Sublobar	Caudate body (R)		8.44	8 8 10
Sublobar	Thalamus ventral ant. (L)		8.05	−6 −6 8
Cerebellum	Declive (R)		4.64	6 −82 −26
Cerebellum	Declive of vermis (L)		5.06	−2 −84 −28
b. Listening to natural speech < Reversed and muffled speech (negative BOLD signal)				
Frontal	Inferior triangular (L)	46	6.14	−46 36 26
Frontal	Middle (L)	10	7.09	−32 46 2
Frontal	Middle (L)	46	7.08	−42 48 10
Frontal	Middle (R)	9	7.72	34 44 38
Frontal	Middle (R)	10	5.98	38 42 8
Frontal	Middle (R)	10	5.89	48 46 22
Frontal	Paracentral (L)	5	5.8	−12 −36 62
Frontal	Precentral (R)	4	5.51	36 −28 66
Occipital	Cuneus (L)	19	5.84	−10 −88 26
Occipital	Superior (L)	19	7	−16 −84 32
Parietal	Inferior (L)	40	6.37	−48 −38 44
Parietal	Inferior (L)	40	6.16	−44 −52 54
Parietal	Inferior (L)	40	5.65	−52 −52 50
Parietal	Postcentral (L)	3	6.37	−22 −36 60
Parietal	Postcentral (R)	4	6.58	36 −30 56
Parietal	Postcentral (R)	40	7.51	60 −22 46
Parietal	Precuneus (L)	7	5.68	−12 −48 60
Parietal	Precuneus (L)	7	5.2	−14 −62 62
Parietal	Precuneus (L)	31	6.25	−24 −76 16
Parietal	Superior (L)	7	4.86	−14 −68 54
Parietal	Superior (L)	7	4.23	−22 −70 58
Parietal	Superior (R)	7	6.27	20 −62 50
Parietal	Superior (R)	7	5.85	14 −74 52
Parietal	Superior (R)	7	5.34	16 −58 56
Parietal	Superior (R)	40	8.37	52 −42 60
Sublobar	Insula (R)	13	6.05	38 −8 −6
Sublobar	Insula (R)	13	5.33	42 −2 4
Sublobar	Insula (R)	13	4.1	38 −10 6

Effective corrected threshold $p \leq 0.02$ for cluster size 40.

connectivity. When the speech was meaningful, the areas of positive BOLD signal decreased their connectivity to the DMN and the areas of negative BOLD signal decreased their connectivity to the traditional language areas in frontal and temporal cortices.

Discussion

These results indicate that engagement of particular activated and/or deactivated regions is related to the nature of the language processes, with language comprehension of

TABLE 3. CHANGES IN CONNECTIVITY FOR THE FRONTOPARIETAL REGIONS WITH NEGATIVE BOLD SIGNAL ASSOCIATED WITH SPEECH DURING THE NATURAL SPEECH IN COMPARISON TO THE REVERSED AND MUFFLED SPEECH

Region	*Anatomical area*	*Brodmann's area*	*T max*	*x*, y, z *(mm)*
a. Increased connectivity during listening to natural speech				
Frontal	Supplementary motor area (R)	6	6.35	0 −12 52
b. Decreased connectivity during listening to natural speech				
Temporal	Superior (L)	21	−7.15	−56 −26 −8
Temporal	Superior (L)	21	−6.56	−50 −40 2
Temporal	Superior (L)	22	−6.09	−58 −30 0
Temporal	Superior (R)	21	−8.31	64 −16 −6
Temporal	Superior (R)	21	−8.21	58 −6 −4
Temporal	Superior (R)	22	−7.71	64 −2 −8
Frontal	Inferior operculum (R)	44	−5.75	52 10 8
Frontal	Inferior triangularis (L)	9	−6.68	−46 16 28
Frontal	Inferior triangularis (L)	45	−6.49	−54 16 24

Effective corrected threshold $p \leq 0.02$ for cluster size 40.

natural intelligible speech engaging a large-scale frontoparietal deactivated signal not observed when the stimuli are unintelligible. The contrast of natural versus muffled and reversed speech demonstrated clusters of positive BOLD signals with respect to the resting baseline within the temporal cortex and frontal cortex that correspond well with current accounts of large-scale networks associated with auditory language comprehension of sentences and syntactic processing located in the temporal and frontal areas (Fiebach et al., 2004; Humphries et al., 2007; Hunter et al., 2006; Saur et al., 2008, 2010; Seghier et al., 2010; Snijders et al., 2010; Papoutsi et al., 2011; Tyler et al., 2011). Current models

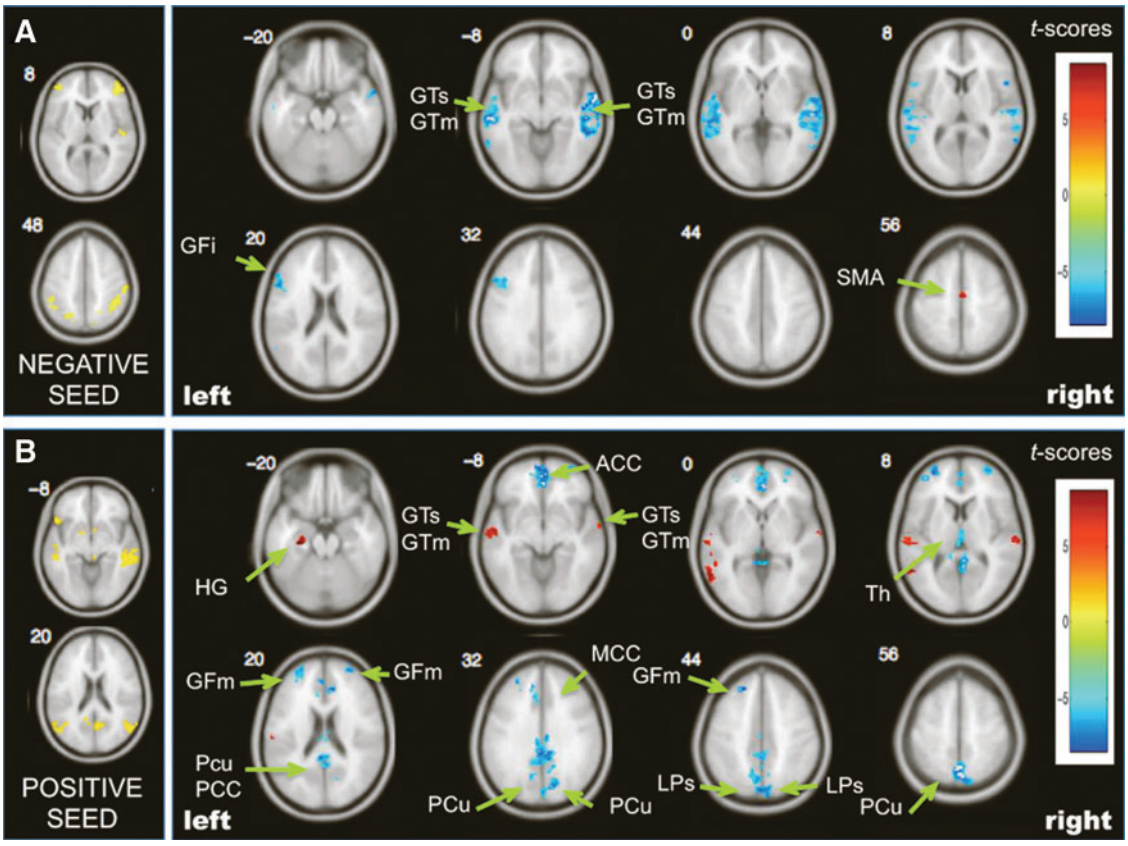

FIG. 3. Psychophysiological interaction results of functional connectivity for the networks associated with language comprehension. Red represents increases in connectivity with the seed network and blue clusters represent decreases in connectivity (effective corrected threshold $p \leq 0.02$ for cluster size 40). **(A)** Changes in connectivity with the negative frontoparietal network seed (shown in yellow in the left panel) for the natural speech in comparison to the muffled and reversed speech. **(B)** Changes in connectivity with the positive regions' network seed (shown in yellow in the left panel) for the natural speech compared to the muffled and reversed speech.

Table 4. Changes in Functional Connectivity for the Language Comprehension Regions with Positive BOLD Signal Associated with Speech During the Natural Speech in Comparison to the Reversed and Muffled Speech

Region	*Anatomical area*	*Brodmann's area*	*T max*	*x*, y, z *(mm)*
a. Increased connectivity during listening to natural speech				
Temporal	Middle (L)	21	7.51	−60 −58 0
Temporal	Middle (L)	21	6.77	−56 −46 4
Temporal	Middle (L)	21	6.29	−58 −10 −8
Temporal	Middle (L)	21	5.29	−66 −34 −6
Temporal	Middle (L)	21	5.12	−58 −32 −4
Temporal	Middle (L)	39	3.93	−52 −56 10
Temporal	Middle (R)	21	5.35	64 −4 −10
Temporal	Superior (R)	22	4.94	66 −10 0
Temporal	Transverse (L)	41	5.8	−44 −24 12
Parietal	Postcentral (R)	40	5.83	64 −20 14
Parietal	Supramarginal (L)	40	6.72	−54 −24 14
Limbic	Hippocampal (L)	35	8.47	−28 −20 −20
b. Decreased connectivity during listening to natural speech				
Frontal	Medial orbital (R)	10	−7.13	8 62 −6
Frontal	Medial orbital (R)	32	−8.33	4 42 −4
Frontal	Middle (L)	10	−7.33	−40 50 8
Frontal	Middle (L)	10	−5.19	−32 46 16
Frontal	Middle (L)	10	−7.2	−24 34 46
Frontal	Middle (L)	10	−5.82	−32 56 4
Frontal	Middle (R)	10	−5.89	30 58 20
Frontal	Middle orbital (R)	10	−6.36	34 60 −8
Frontal	Superior (L)	8	−4.08	−12 36 38
Frontal	Superior (L)	10	−7.17	−26 46 28
Frontal	Superior (L)	10	−6.4	−24 56 14
Frontal	Superior (R)	10	−6.03	32 62 12
Frontal	Superior medial (L)	9	−7.76	−4 44 24
Limbic	Posterior cingulate (R)	30	−8.01	2 −52 12
Limbic	Posterior cingulate (R)	31	−7.9	0 −38 30
Limbic	Posterior cingulate (R)	31	−7.88	4 −44 10
Occipital	Cuneus (R)	7	−9.89	20 −70 28
Parietal	Precuneus (L)	7	−7.69	−2 −62 56
Parietal	Precuneus (L)	7	−5.25	−12 −64 30
Parietal	Precuneus (R)	7	−11.37	4 −60 62
Sublobar	Thalamus medial dorsal (R)		−4.71	2 −12 6
Sublobar	Thalamus (R)		−8.54	6 −16 16

Effective corrected threshold $p \leq 0.02$ for cluster size 40.

associate language processing with larger networks with components in temporal, frontal gyrus, and subcortical regions (Barbas et al., 2013; Catani et al., 2005; Friederici, 2009; Hirsch et al., 2000; Kelly et al., 2010; Papoutsi et al., 2011; Saur et al., 2008; Xiang et al., 2010). Neuroimaging studies confirm that mapping phonological representations onto lexical conceptual representations involves the anterior superior temporal, middle temporal, and inferior temporal sulcus that connect to premotor areas (BA 44 and 6) (Warren et al., 2009). In addition, semantic processing engages the superior temporal sulcus and the superior temporal gyrus, as well as the middle temporal gyrus connecting to the ventrolateral prefrontal cortex (BA 45 and 47) (Saur et al., 2010; Vigneau et al., 2006; Weiller et al., 2011).

The authors also observed strong positive activation of hippocampal and parahippocampal gyrus during language comprehension that is paired with activation of the precuneus/PCC suggesting the engagement of memory functions as well. The posterior inferior parietal lobule and the precuneus have been associated with episodic memory retrieval (Huijbers et al., 2012; Shannon and Buckner, 2004). The positive time course for meaningful speech and negative signal for muffled speech in the posterior cingulate gyrus and precuneus is in agreement with the role of this region in semantic processing observed by Seghier and Price (2012). A meta-analysis of 120 studies points to the role of precuneus/PCC as an interface between the semantic network and the hippocampal memory system to encode meaningful events into episodic memory (Binder and Desai, 2011). On the other hand, the hippocampus and adjacent areas in the medial temporal lobe that are associated with episodic memory function are also part of the DMN (Greicius and Menon, 2004). In fact, hippocampal formation shows spontaneous correlations with many of the major regions of the DMN (Vincent et al., 2008). In this study, the hippocampal gyrus (slice −20) is active in two contrasts: all speech conditions versus resting baseline (Fig. 1) and meaningful speech (forward speech vs. reversed and muffled speech, slice −20). These results indicate that the signal amplitude for forward speech is greater than for the other speech conditions, although all conditions

have a positive signal in this region. Therefore, hippocampal activation may be related to recollection associated with intelligibility of speech that brings back memories, but it could also be related to recollection associated to other attributes of the stimuli (i.e., recognition of a familiar voice, emotional recollection associated to it). On the other hand, parahippocampal gyrus and a region of the hippocampus are also deactivated for all speech conditions versus resting baseline (Fig. 1, slices −8 and 0), suggesting that the signal is below the resting baseline for all the conditions to some degree. Therefore, these regions do not decrease activation with the intelligibility of the speech as the areas shown in Figure 2. The results show a heterogeneity of subregions of the hippocampal gyrus regarding activation or deactivation during language comprehension. Although this study was not designed to disentangle the precise roles of these structures for language comprehension, the different patterns of activation suggest a different contribution of these subregions of the hippocampal system to episodic memory associated with language processing.

The contrast of natural versus muffled and reversed speech also demonstrated clusters of negative BOLD signals with respect to the resting baseline. Notably, negative BOLD responses with respect to the resting baseline have not been consistently reported in language studies possibly because this signal is smaller than the positive BOLD signal for a similar change of neural activity (Shmuel et al., 2006). The negative BOLD signals with respect to the resting baseline observed in this study encompass the intraparietal sulcus, parietal and the insular regions; areas that have been described as a dorsal attention network activated during externally oriented tasks (Corbetta, 1998; Fox et al., 2005; Gazzaley et al., 2007) and have also been associated with a control network that responds to cues that indicate task onset (Dosenbach et al., 2008). Dosenbach and colleagues (2008) have proposed that this network encompasses regions that initiate attentional control triggered by the cue and regions that process trial-by-trial performance feedback to adjust control. Based on these studies, the authors expected the frontal parietal network to be silent in the absence of an explicit task. Furthermore, they expected this network to be active during the presentation of the muffled and reversed speech due to the greater effort of processing these unusual stimuli. However, the deactivation of these regions during passive listening to natural speech suggests a different engagement. This result could be interpreted as a suppression of the attention network, but further investigation is necessary.

It has been widely shown that cerebral activity is coupled with the positive BOLD responses by localized changes in blood oxygenation that produce a mismatch of changes in the cerebral blood flow (CBF), cerebral blood volume (CBV), and cerebral metabolic rate of oxygen consumption ($CMRO_2$) (Kim and Ogawa, 2012). Positive BOLD responses correlate with increases in CBV and CBF. However, the neuronal origin of the negative BOLD signal appears to be less understood. The coupling with decreases of CBF and $CMRO_2$ is supported by many studies (Blumenfeld et al., 2004; Englot et al., 2009; Mullinger et al., 2014; Shmuel et al., 2002) suggesting that the intrinsic dynamics serve cognitive and perceptual processes (Shmuel et al., 2002, 2006). However, negative BOLD signals do not necessarily reflect decreased CBF associated with neural activity. The signal polarity can also be explained by a decrease of CBF due to a redistribution of CBF into neighboring regions that causes a local decrease of CBF (known as the vascular steal effect) (Harel et al., 2002; Kannurpatti and Biswal, 2004). Other possible mechanisms include a large increase in $CMRO_2$ without an adequate CBF increase in areas with low vascular reactivity (Schridde et al., 2008), or an increase of dopamine release that causes an increased activity of subcortical structures and vasoconstriction of neighboring microvessels (Shih et al., 2009). Therefore, the hemodynamic mechanism may be different for positive and negative BOLD signals. The techniques employed in this study do not differentiate between these possible underlying mechanisms. Finally, negative BOLD signals have been observed in caudate and putamen despite their increased neural activity during spontaneous seizures (Mishra et al., 2011). Therefore, caution must be used in the interpretation of the negative BOLD signal for these structures and in cases of altered hemodynamics in brain pathologies.

The observed negative and positive signals observed during language comprehension might be interpreted as cooperative and separate processes. In this frame, the negative signals in the absence of goal-directed tasks might allow for a more efficient processing of the auditory information, and to a greater extent when the speech is meaningful. The authors observed that regions specific for processing natural intelligible language exert both an enhancement of functional connectivity on traditional language regions and a weakening of functional connectivity to the deactivated areas during speech comprehension. This may serve to reduce interference with other processes.

Alternatively, the meaningful auditory stimuli, selectively engaging the posterior tempoparietal cortex and posterior cingulate gyrus, could amplify neural representations of task-relevant information while disengaging from representations of task-irrelevant information in frontoparietal signals. Amplification of the brain response to task-relevant information has been previously shown in cognitive control paradigms (Chadick and Gazzaley, 2011; Egner and Hirsch, 2005). These effects could be applied directly from the posterior temporal or the PCC or mediated by subcortical areas such as the thalamus or insular cortex.

Binder and colleagues (1999) suggested that if the observed deactivations relative to the resting baseline were due to the relocation of resources, their amplitudes would be expected to vary with task difficulty. In this study, the authors used natural speech and two unintelligible versions of the same auditory stimuli to isolate brain regions that process meaning and observed a variation of the positive BOLD signal relative to the resting baseline for the three speech conditions, but without a similar variation in the negative signal. However, a further variation in the level of speech comprehension may be necessary to assess the responsiveness of the BOLD signal and could be the target of future studies to investigate factors that affect brain regions with negative BOLD signals outside the DMN.

The observation of both positive and negative signals relative to the resting baseline only for natural speech suggests a possible interaction between positive and negative signals during high-level (meaningful) language processing. Functional connectivity using an inclusive seed composed of all the regions of positive BOLD signals, mainly composed by

canonical language areas in the superior/middle temporal and inferior frontal gyri, showed increased connectivity with auditory and language regions of the temporal cortex. These findings are in agreement with reported increased connectivity between the left posterior temporal cortex and left inferior frontal gyrus, bilateral middle temporal, left posterior inferior temporal gyrus, and right occipital gyrus comparing ambiguous and unambiguous sentences (Snijders et al., 2010). Papoutsi and colleagues (2011) found only negative PPI effects for ambiguous compared to unambiguous sentences. Coupling was observed between the left posterior middle temporal and bilateral anterior cingulate cortex/medial frontal gyrus, precuneus and left middle occipital gyrus. Similarly, the authors found strong decreases in connectivity from the canonical language areas to medial regions of the DMN. On the other hand, functional connectivity using an inclusive seed composed of all the regions of negative BOLD signal, mainly composed of frontoparietal areas in the middle frontal gyrus and superior and inferior parietal areas, showed decreased connectivity to temporal and frontal speech processing regions and increased connectivity only to the SMA. The SMA was deactivated during the contrast of all conditions against baseline.

These global connectivity patterns suggest that regions with negative and positive BOLD signals relative to the resting baseline dynamically decrease their connectivity during speech comprehension, coupled with functional changes in connectivity to the deactivated regions that are considered part of the DMN. Thus, the neural dynamics of language comprehension include both strengthening connectivity between positive BOLD regions and temporal regions and decreasing connectivity between positive BOLD regions and DMN regions and between negative fronto-parietal network and traditional language areas.

Conclusion

The authors test the hypothesis that large-scale networks of negative signals relative to a resting baseline are a fundamental component of the neural underpinnings of speech comprehension, and that the neural dynamics of language comprehension involve interactions between large-scale networks, including both positive and negative anticorrelated signals. In this study, fMRI was employed to acquire neural responses during listening to meaningful natural speech in comparison to incomprehensible versions of the same speech. An extensive temporal-frontal language network of areas with positive signals relative to the resting baseline was observed as expected. Furthermore, negative signals relative to the resting baseline were observed in the frontoparietal regions associated specifically with speech comprehension. These findings demonstrate that receptive language-induced negative BOLD signals are anticorrelated with the receptive language-induced positive BOLD signals during comprehension of spoken language. The anticorrelation between positive and negative BOLD signals relative to the resting baseline is observed during the intelligible natural speech and not during the unintelligible speech. Thus, both distinct positive and negative signal responses are observed in the contrast of speech against baseline and in the contrast of natural speech against muffled and reversed speech. These results suggest that the differences between processing meaningful intelligible speech and unintelligible speech are not only shown by patterns of positive signals but also that the patterns of negative signals reflect processes also contributing to the processing of language stimuli. While the language regions with positive BOLD signals relative to the resting baseline increased connectivity to adjacent temporal areas and decreased connectivity to the medial areas typically associated to the DMN, the frontoparietal regions with negative BOLD signals relative to the resting baseline decreased their connectivity to temporal and frontal language areas. These findings suggest that the neural dynamics of processing natural speech include specific strengthening and weakening of connectivity between networks of positive and negative BOLD signals, consistent with a model of large-scale anticorrelated processes in language comprehension.

Understanding the functional relationships between positive and negative BOLD signals relative to the resting baseline could further the understanding of language deficits of neurological origin such as autism and acquired language deficits such as disorders of consciousness (Rodriguez Moreno et al., 2010). The passive task employed in this study allows natural listening without imposing laboratory-constrained conditions. The personalized natural narrative segments used in this paradigm motivates future applications to clinical situations where the ability to respond is impaired. Subjects were asked to attend to the narratives with their eyes closed, and comprehension of the natural narratives was confirmed for all imaging runs and failure to comprehend was confirmed for the muffled and reversed conditions. Language conditions that impose minimal attention requirements such as the passive listening have been used for patients who have limited cognitive or motor abilities, and this utility provides an additional rationale for studying the fundamental properties of language comprehension using a passive listening paradigm.

Acknowledgment

This work was supported, in part, by the National Institutes of Health (1R01HD051912 to N.D.S. and J.H.).

Author Disclosure Statement

No competing financial interests exist.

References

Ackermann H, Riecker A. 2010. The contribution(s) of the insula to speech production: a review of the clinical and functional imaging literature. Brain Struct Funct 214:419–433.

Anderson JS, Ferguson MA, Lopez-Larson M, Yurgelun-Todd D. 2011. Connectivity gradients between the default mode and attention control networks. Brain Connect 1:147–157.

Anticevic A, Repovs G, Shulman GL, Barch DM. 2010. When less is more: TPJ and default network deactivation during encoding predicts working memory performance. Neuroimage 49:2638–2648.

Barbas H, Garcia-Cabezas MA, Zikopoulos B. 2013. Frontal-thalamic circuits associated with language. Brain Lang 126:49–61.

Binder J, et al. 1999. Conceptual processing during the conscious resting state. A functional MRI study. J Cogn Neurosci 11:80–95.

Binder JR, Desai RH. 2011. The neurobiology of semantic memory. Trends Cogn Sci 15:527–536.

Binder JR, Medler DA, Desai R, Conant LL, Liebenthal E. 2005. Some neurophysiological constraints on models of word naming. Neuroimage 27:677–693.

Biswal B, Zerrin Yetkin F, Haughton VM, Hyde JS. 1995. Functional connectivity in the motor cortex of resting human brain using echo-planar MRI. Magn Reson Med 34:537–541.

Blumenfeld H, et al. 2004. Positive and negative network correlations in temporal lobe epilepsy. Cereb Cortex 14:892–902.

Buckner RL, Andrews-Hanna JR, Schacter DL. 2008. The brain's default network: anatomy, function, and relevance to disease. Ann N Y Acad Sci 1124:1–38.

Buckner RL, Raichle ME, Miezin FM, Petersen SE. 1996. Functional anatomic studies of memory retrieval for auditory words and visual pictures. J Neurosci 16:6219–6235.

Catani M, Jones DK, ffytche DH. 2005. Perisylvian language networks of the human brain. Ann Neurol 57:8–16.

Chadick JZ, Gazzaley A. 2011. Differential coupling of visual cortex with default or frontal-parietal network based on goals. Nat Neurosci 14:830–832.

Corbetta M. 1998. Frontoparietal cortical networks for directing attention and the eye to visual locations: identical, independent, or overlapping neural systems? Proc Natl Acad Sci U S A 95:831–838.

Diaz MT, McCarthy G. 2009. A comparison of brain activity evoked by single content and function words: an fMRI investigation of implicit word processing. Brain Res 1282:38–49.

Dosenbach NU, Fair DA, Cohen AL, Schlaggar BL, Petersen SE. 2008. A dual-networks architecture of top-down control. Trends Cogn Sci 12:99–105.

Egner T, Hirsch J. 2005. Cognitive control mechanisms resolve conflict through cortical amplification of task-relevant information. Nat Neurosci 8:1784–1790.

Englot DJ, et al. 2009. Cortical deactivation induced by subcortical network dysfunction in limbic seizures. J Neurosci 29:13006–13018.

Fiebach CJ, Vos SH, Friederici AD. 2004. Neural correlates of syntactic ambiguity in sentence comprehension for low and high span readers. J Cogn Neurosci 16:1562–1575.

Fox MD, Raichle ME. 2007. Spontaneous fluctuations in brain activity observed with functional magnetic resonance imaging. Nat Rev Neurosci 8:700–711.

Fox MD, Snyder AZ, et al. 2005. The human brain is intrinsically organized into dynamic, anticorrelated functional networks. Proc Natl Acad Sci U S A 102:9673–9678.

Friederici AD. 2009. Pathways to language: fiber tracts in the human brain. Trends Cogn Sci 13:175–181.

Friston KJ, et al. 1997. Psychophysiological and modulatory interactions in neuroimaging. NeuroImage 6:218229.

Gazzaley A, et al. 2007. Functional interactions between prefrontal and visual association cortex contribute to top-down modulation of visual processing. Cereb Cortex 17 Suppl 1:i125–i135.

Greicius MD, Menon V. 2004. Default-mode activity during a passive sensory task: uncoupled from deactivation but impacting activation. J Cogn Neurosci 16:1484–1492.

Gusnard DA, Raichle ME, Raichle ME. 2001. Searching for a baseline: functional imaging and the resting human brain. Nat Rev Neurosci 2:685–694.

Harel N, Lee SP, Nagaoka T, Kim DS, Kim SG. 2002. Origin of negative blood oxygenation level-dependent fMRI signals. J Cereb Blood Flow Metab 22:908–917.

Hirsch J, et al. 2000. An integrated functional magnetic resonance imaging procedure for preoperative mapping of cortical areas associated with tactile, motor, language, and visual functions. Neurosurgery 47:711–721; discussion 721–722.

Huijbers W, et al. 2012. Explaining the encoding/retrieval flip: memory-related deactivations and activations in the posteromedial cortex. Neuropsychologia 50:3764–3774.

Humphries C, Binder JR, Medler DA, Liebenthal E. 2007. Time course of semantic processes during sentence comprehension: an fMRI study. Neuroimage 36:924–932.

Hunter MD, et al. 2006. Neural activity in speech-sensitive auditory cortex during silence. Proc Natl Acad Sci U S A 103:189–194.

Kannurpatti SS, Biswal BB. 2004. Negative functional response to sensory stimulation and its origins. J Cereb Blood Flow Metab 24:703–712.

Kelly C, et al. 2010. Broca's region: linking human brain functional connectivity data and non-human primate tracing anatomy studies. Eur J Neurosci 32:383–398.

Kim SG, Ogawa S. 2012. Biophysical and physiological origins of blood oxygenation level-dependent fMRI signals. J Cereb Blood Flow Metab 32:1188–1206.

Mazoyer B, et al. 2001. Cortical networks for working memory and executive functions sustain the conscious resting state in man. Brain Res Bull 54:287–298.

McKiernan KA, Kaufman JN, Kucera-Thompson J, Binder JR. 2003. A parametric manipulation of factors affecting task-induced deactivation in functional neuroimaging. J Cogn Neurosci 15:394–408.

Mechelli A, Gorno-Tempini ML, Price CJ. 2003. Neuroimaging studies of word and pseudoword reading: consistencies, inconsistencies, and limitations. J Cogn Neurosci 15:260–271.

Mishra AM, et al. 2011. Where fMRI and electrophysiology agree to disagree: corticothalamic and striatal activity patterns in the WAG/Rij rat. J Neurosci 31:15053–15064.

Mullinger KJ, Mayhew SD, Bagshaw AP, Bowtell R, Francis ST. 2014. Evidence that the negative BOLD response is neuronal in origin: a simultaneous EEG-BOLD-CBF study in humans. Neuroimage 94:263–274.

Papoutsi M, Stamatakis EA, Griffiths J, Marslen-Wilson WD, Tyler LK. 2011. Is left fronto-temporal connectivity essential for syntax? Effective connectivity, tractography and performance in left-hemisphere damaged patients. Neuroimage 58:656–664.

Price CJ. 2012. A review and synthesis of the first 20 years of PET and fMRI studies of heard speech, spoken language and reading. Neuroimage 62:816–847.

Rissman J, Eliassen JC, Blumstein SE. 2003. An event-related FMRI investigation of implicit semantic priming. J Cogn Neurosci 15:1160–1175.

Rodriguez Moreno D, Schiff ND, Giacino J, Kalmar K, Hirsch J. 2010. A network approach to assessing cognition in disorders of consciousness. Neurology 75:1871–1878.

Saur D, et al. 2008. Ventral and dorsal pathways for language. Proc Natl Acad Sci U S A 105:18035–18040.

Saur D, et al. 2010. Combining functional and anatomical connectivity reveals brain networks for auditory language comprehension. Neuroimage 49:3187–3197.

Schafer RJ, Constable T. 2009. Modulation of functional connectivity with the syntactic and semantic demands of a Noun Phrase Formation Task: a possible role for the Default Network. Neuroimage 46:882–890.

Schridde U, et al. 2008. Negative BOLD with large increases in neuronal activity.'' Cereb Cortex 18:1814–1827.

Seghier ML, Fagan E, Price CJ. 2010. Functional subdivisions in the left angular gyrus where the semantic system meets and diverges from the default network. J Neurosci 30:16809–16817.

Seghier ML, Price CJ. 2009. Dissociating functional brain networks by decoding the between-subject variability. Neuroimage 45:349–359.

Seghier ML, Price CJ. 2012. Functional heterogeneity within the default network during semantic processing and speech production. Front Psychol 3:281.

Sestieri C, Corbetta M, Romani GL, Shulman GL. 2011. Episodic memory retrieval, parietal cortex, and the default mode network: functional and topographic analyses. J Neurosci 31:4407–4420.

Shannon BJ, Buckner RL. 2004. Functional-anatomic correlates of memory retrieval that suggest nontraditional processing roles for multiple distinct regions within posterior parietal cortex. J Neurosci 24:10084–10092.

Shih YY, et al. 2009. A new scenario for negative functional magnetic resonance imaging signals: endogenous neurotransmission. J Neurosci 29:3036–3044.

Shmuel A, Augath M, Oeltermann A, Logothetis NK. 2006. Negative functional MRI response correlates with decreases in neuronal activity in monkey visual area V1. Nat Neurosci 9:569–577.

Shmuel A, Yacoub E, et al. 2002. Sustained negative BOLD, blood flow and oxygen consumption response and its coupling to the positive response in the human brain. Neuron 36:1195–1210.

Shulman GL, et al. 1997. Common blood flow changes across visual tasks: II. decreases in cerebral cortex. J Cogn Neurosci 9:648–663.

Snijders TM, Petersson KM, Hagoort P. 2010. Effective connectivity of cortical and subcortical regions during unification of sentence structure. NeuroImage 52:1633–1644.

Snijders TM, Vosse T, et al. 2009. Retrieval and unification of syntactic structure in sentence comprehension: an FMRI study using word-category ambiguity. Cereb Cortex 19: 1493–1503.

Tyler LK, et al. 2011. Left inferior frontal cortex and syntax: function, structure and behaviour in patients with left hemisphere damage. Brain 134(Pt 2):415–431.

Uddin LQ, Kelly AM, Biswal BB, Castellanos FX, Milham MP. 2009. Functional connectivity of default mode network components: correlation, anticorrelation, and causality. Hum Brain Mapp 30:625–637.

Vigneau M, et al. 2006. Meta-analyzing left hemisphere language areas: phonology, semantics, and sentence processing. NeuroImage 30:1414–1432.

Vincent JL, Kahn I, Snyder AZ, Raichle ME, Buckner RL. 2008. Evidence for a frontoparietal control system revealed by intrinsic functional connectivity. J Neurophysiol 100:3328–3342.

Warren JE, Crinion JT, Lambon Ralph MA, Wise RJ. 2009. Anterior temporal lobe connectivity correlates with functional outcome after aphasic stroke. Brain 132(Pt 12):3428–3442.

Weiller C, Bormann T, Saur D, Musso M, Rijntjes M. 2011. How the ventral pathway got lost: and what its recovery might mean. Brain Lang 118:29–39.

Xiang HD, Fonteijn HM, Norris DG, Hagoort P. 2010. Topographical functional connectivity pattern in the perisylvian language networks. Cereb Cortex 20:549–560.

Xiao Z, et al. 2005. Differential activity in left inferior frontal gyrus for pseudowords and real words: an event-related fMRI study on auditory lexical decision. Hum Brain Mapp 25:212–221.

Yoncheva YN, Zevin JD, Maurer U, McCandliss BD. 2010. Auditory selective attention to speech modulates activity in the visual word form area. Cereb Cortex 20:622–632.

Zekveld AA, Heslenfeld DJ, Festen JM, Schoonhoven R. 2006. Top-down and bottom-up processes in speech comprehension. Neuroimage 32:1826–1836.

Address correspondence to
Joy Hirsch
Departments of Psychiatry and Neurobiology
Yale School of Medicine
300 George St.
Suite 902
New Haven, CT 06511

E-mail: joy.hirsch@yale.edu